Donor Variability in Growth Kinetics of Healthy hMSCs Using Manual Processing: Considerations for Manufacture of Cell Therapies

Giulia Detela, Owen W. Bain, Hae-Won Kim, David J. Williams, Chris Mason, Anthony Mathur, and Ivan B. Wall*

Human mesenchymal stromal cells (hMSCs) are excellent candidates for cell therapy but their expansion to desired clinical quantities can be compromised by ex vivo processing, due to differences between donor material and process variation. The aim of this article is to characterize growth kinetics of healthy baseline "reference" hMSCs using typical manual processing. Bone-marrow derived hMSCs from ten donors are isolated based on plastic adherence, expanded, and analyzed for their growth kinetics until passage 4. Results indicate that hMSC density decreases with overall time in culture ($p < 0.001$) but no significant differences are observed between successive passages after passage 1. In addition, fold increase in cell number dropped between passage 1 and 2 for three batches, which correlated to lower performance in total fold increase and expansion potential of these batches, suggesting that proliferative ability of hMSCs can be predicted at an early stage. An indicative bounded operating window is determined between passage 1 and 3 (PDL < 10), despite the high inter-donor variability present under standardized hMSC expansion conditions used. hMSC growth profile analysis will be of benefit to cell therapy manufacturing as a tool to predict culture performance and attainment of clinically-relevant yields, therefore stratifying the patient population based on early observation.

1. Introduction

Human mesenchymal stromal cells (hMSCs) are attractive candidates for a wide number of cell-based therapies due to their multi-modal properties. They are able to differentiate along mesenchymal lineages and can stimulate host tissue regeneration in a paracrine fashion.[1,2]

Although the primary source for derivation is the bone marrow, hMSCs account only for the 0.001–0.01% of the total mononuclear cells present in that tissue[3] and their frequency declines with aging.[2] This is of major significance, given that most hMSC-based therapies are likely to be required for medical conditions that increase in prevalence with increasing age. Therefore, to obtain clinically relevant yields of cell product for autologous cell therapy (which vary greatly from 10^6–10^8 cells per patient depending on injection site and treated indication), the first bioprocessing substantial challenge is the ex vivo expansion of hMSCs that retain desired functional properties (e.g., differentiation and paracrine ability), while limiting the

Dr. G. Detela, Dr. O. W. Bain, Prof. C. Mason, Prof. I. B. Wall
Department of Biochemical Engineering
University College London
Gordon Street, WC1H 0AH
London, United Kingdom
E-mail: i.wall@ucl.ac.uk; i.wall@aston.ac.uk

Prof. H.-W. Kim, Prof. I. B. Wall
Department of Nanobiomedical Science
and BK21 Plus NBM Global Research Center for
Regenerative Medicine
Dankook University
Cheonan 31116, Republic of Korea

Prof. H.-W. Kim
College of Dentistry and Institute of Tissue
Regeneration Engineering (ITREN)
Dankook University
Cheonan 31116, Republic of Korea

Prof. D. J. Williams
Centre for Biological Engineering
Wolfson School of Mechanical and Manufacturing Engineering
Loughborough University
Loughborough LE11 3TU, United Kingdom

Prof. A. Mathur
Barts Health NIHR Biomedical Research Unit
Department of Cardiology
London Chest Hospital
London E2 9JX, United Kingdom

Prof. I. B. Wall
School of Life and Health Sciences
Aston University
Aston Triangle B4 7ET,
Birmingham, United Kingdom

**ADVANCED
SCIENCE NEWS**
www.advancedsciencenews.com

**Biotechnology
Journal**
www.biotechnology-journal.com

impact of the heterogeneity present among different individuals hMSCs. Further, a standardized manufacturing with a process window capable of accommodating input variations due to differences in starting materials is required. Being able to quantify expansion potential in vitro is important for understanding which subsets of patients are likely to benefit therapeutically, based on producing enough cells. Subsequently being able to stratify patients on that basis will improve clinical trial outcomes and reduce overall therapy development costs.

Many protocols exist for hMSC harvest, seeding density, and expansion, yielding significant differences in expansion and functional properties.[4] The conventional procedure for bone marrow-derived hMSCs involves direct establishment of cultures from total tissue aspirates, starting with density centrifugation of the mononuclear cell population and hMSC selection by adherence to plastic. Alternative methods may include immunomagnetic selection based on cell surface marker presence.[5] Once adhered, proliferating hMSCs have a spindle-like morphology and are composed by multiple stromal progenitor cells.[6]

The ISCT criteria defined hMSCs based on the adherence to cell culture plastic, surface marker profile, and capacity to undergo tri-lineage differentiation in vitro.[7] Moreover, additional markers are routinely used to identify bone marrow hMSCs, including CD44/HCAM,[8] STRO-1,[9] and CD146/MCAM.[10,11]

hMSC expansion potential is limited under standard manual processing, to the extent that changes in growth rate and the associated changes in identity and potency render hMSC therapeutic value questionable beyond five passages,[12,13] or beyond 20 population doublings (PDs),[14] with PDs being considered a more reliable and accurate indicator of cell age. As autologous cell products for diseases with systemic causes may yield hMSCs whose quality varies according to the patient severity of the disease, it can be even more difficult to define robust bioprocesses for autologous hMSCs because of biologic variation between patients.[14]

Before trying to create processes that can accommodate poor quality cells from diseased individuals, it is necessary to develop processes using hMSCs from healthy donors, to define whether that process can accommodate variability across healthy donors. Insights gained will then prove useful when screening patients to identify who will likely not benefit from autologous hMSC transplantation due to poor cell expansion potential. Therefore, the aim of this study was to indicate the degree of variability in hMSC growth kinetics across multiple healthy donors when using manual processing that is typical for autologous hMSCs.

2. Experimental Section

2.1. Human Bone Marrow Mesenchymal Stromal Cell Isolation

Cryopreserved bone marrow bags were received from 10 human male donors, aged between 16 and 18. The Research Ethics Committee (REC) responsible was Central London REC 4 and the Joint UCL/UCLH Ethic Committee Reference

Number for the project is REC 03/0136. Each bag contained 80–120 mL of aspirate. The following procedure refers to an aspirate of 100 mL. Thawed bone marrow was diluted with 100 mL of $1\times$ Ca^{2+}/Mg^{2+}-free sterile PBS (Sigma–Aldrich, Poole, UK) containing 1% Anti/Anti (Invitrogen, Paisley, UK). A total of 20 mL suspension aliquots were added to the surface of 30 mL of Ficoll-Paque PLUS (GE Healthcare, Little Chalfont, UK). Centrifugation was performed at 650g for 30 min at 20 °C without acceleration and brakes. The mononuclear cell phases were washed by centrifugation for 15 min with a total of 120–150 mL sterile $1\times$ PBS/5% Anti/Anti. Cell pellets were pooled in complete medium, formulated with low glucose DMEM (supplemented with Glutamax, Sodium Pyruvate, and Phenol Red, Invitrogen), 10% FBS (Sera Laboratories International, Haywards Heath, UK), 1 ng mL^{-1} recombinant hFGF-2 (R&D Systems, Minneapolis, MN, USA) and 1% Anti/Anti. Cells were seeded at 1×10^4 cells/cm^2 density in T75 flasks (Nunc, Roskinlde, Denmark) and maintained in atmospheric oxygen in a 5% CO_2 humidified incubator.

2.2. hMSC Expansion

hMSCs were maintained in culture with 15–20 mL of complete medium/T75 flask. Non-adherent cells were removed on day 6. The first visible hMSC colonies were labelled as passage 0 (p0). Complete medium was replaced every 3 days at each passage. Daily observation of the cultures was performed with an inverted light microscope (Eclipse50i, Nikon). Once p0 hMSCs reached $\approx$90% confluence, they were detached using 0.25% trypsin/EDTA (Sigma–Aldrich), counted using a hemocytometer and plated into passage 1 (p1). Passaging was performed according to a 1:3 ratio and expansion was carried throughout the end of passage 4 (p4).

2.3. Tri-lineage Differentiation

p2 hMSCs were induced in 12-well plates (Corning, NY, USA) using commercial differentiation medium. All cultures were fed every 3 days with 1 mL of differentiation medium. Control hMSCs cultures were processed in parallel using complete medium.

2.3.1. Adipogenic Differentiation

hMSCs were seeded at 1×10^4 cells/cm^2 in complete growth medium for 2 h. Cells were washed in $1\times$ PBS and Adipogenesis Differentiation Medium (StemPro Adipogenesis Differentiation Kit, Invitrogen) was added. On day 14 cells were washed in $1\times$ PBS and fixed at room temperature for 10 min with 4% PFA (Sigma–Aldrich). Cells were rinsed with distilled water, then permeabilized with 60% isopropanol (VWR International Ltd, Poole, UK) for 5 min and stained with a filtered solution of 0.3% w/v Oil Red O (Sigma–Aldrich)/isopropanol in distilled water 3:2 for 5 min, rinsed under tap water and counterstained with hematoxylin (Sigma–Aldrich).

**ADVANCED
SCIENCE NEWS**
www.advancedsciencenews.com

**Biotechnology
Journal**
www.biotechnology-journal.com

2.3.2. Osteogenic Differentiation

hMSCs were seeded at 5×10^3 cells/cm^2 with complete medium for 2 h. The medium was replaced with Osteogenesis Differentiation Media (StemPro Osteogenesis Differentiaiton Kit, Invitrogen). On day 21, they were washed in $1\times$ PBS, fixed with 4% PFA for 30 min at room temperature and rinsed with distilled water. A 2% Alizarin Red S solution (Sigma–Aldrich) at pH 4.2 was added for 5 min prior to rinsing with distilled water.

2.3.3. Chondrogenic Differentiation

hMSCs micromasses were generated by seeding $10\,\mu$L of a 1.6×10^7 hMSC/mL suspension in a well of a 12-well plate. After 4 h, Chondrogenesis Differentiation Media (StemPro Chondrogenesis Differentiaiton Kit, Invitrogen) was added. On day 14 cells were washed in $1\times$ PBS, fixed at room temperature for 30 min with 4% PFA, rinsed and stained in 1% Alcian Blue solution (Sigma–Aldrich) prepared in 0.1 M HCl (Sigma–Aldrich) for 30 min. Cells were rinsed twice in 0.1 M HCL and then with distilled water.

2.4. Immunocytochemistry

p2 hMSCs were washed with PBS, fixed in 4% PFA for 10 min, and incubated in blocking solution (1% BSA [Sigma–Aldrich] in PBS) for 1 hr at room temperature. Primary antibodies were used 1:100 in blocking solution overnight at 4 °C. Cells were washed in blocking solution three times. Secondary antibodies were used 1:300 in PBS for 45 min. Nuclei were counterstained with DAPI (Life Technologies, Paisley, UK) 1:10 000 in PBS for 5 min. All primary antibodies (α-CD14: Mouse IgG1, MAB1219; α-CD19: Mouse IgG2a, MAB1794; α-CD34: Mouse IgG1, MAB4211; α-CD44 (H-CAM): Mouse IgG2a, CBL154; α-CD45: Mouse IgG2a, 05-1410; α-CD73: Mouse IgG1K, MABD122; α-CD90: Mouse IgG1, CBL415; α-CD105: Mouse IgG2a, 05-1424; α-CD146 (M-CAM): Mouse IgG1, MAB16985; α-STRO-1: Mouse IgM, MAB4315) were purchased from Millipore, UK, secondary antibodies (Donkey α-Mouse IgG: A-31570 and Goat α-Mouse IgM: A-21042) from Life Technologies.

2.5. Flow Cytometry

p2 and p3 hMSCs were characterized using MSC Phenotyping Kit (MACS, Miltenyi Biotec). Briefly, 5×10^5 hMSC aliquots were resuspended in $100\,\mu$L of buffer (PBS $1\times$, pH 7.2, 0.5% BSA, 2 mM EDTA) and incubated at room temperature for 40 min. Following compensation, hMSCs were analyzed on BD FACSCalibur (Becton Dickinson) at the Scientific Support Services Facility of UCL Cancer Institute and Wolfson Institute for Biomedical Research. Results were plotted with Summit v4.3 Software (Beckman Coulter Inc., Brea, CA, USA).

2.6. Determination of Growth Kinetics

Proliferation was assessed via Trypan Blue (Sigma–Aldrich) exclusion for each hMSC batch at each passage.

2.6.1. Doubling Time (T_d)

Growth rate was measured for every batch between p1 and p4 and expressed in hours as T_d, using $(T-T_0)*\log(2)/\log(N/N_0)$, where $T =$ total hours at harvest and $T_0 =$ hours at passage initiation, $N =$ total confluent hMSC number and $N_0 =$ total initial hMSC number.

2.6.2. Cell Density

Cell density was calculated as confluent hMSC number over the growth area in cm^2.

2.6.3. Calculation of Population Doubling Level (PDL)

Growth rate was also measured for every batch between p0 and p4 as PDL, using $(\log N - \log N_0)/\log 2$, where $N =$ confluent hMSC number and $N_0 =$ seeded hMSC number.

2.6.4. Fold Increase in Cell Number

This was calculated as the total hMSCs at p4 over the number of total hMSCs at p0. Similarly, serial fold increase in cell number was calculated as cell yield of each given passage number over cell yield of the previous passage number.

2.6.5. Expansion Potential

The growth rate that could potentially be reached at each passage, provided the entire hMSC population from each donor was processed, was calculated based on cell density at passage, multiplied for the total growth area in cm^2 according to a 1:3 splitting ratio.

2.7. Statistical Analysis

Each batch was expanded one time and duplicate measurements were performed on the same material. Results are presented as mean $\pm$ standard deviation for individual hMSC donors and for averaged data from all 10 donors, to represent inter-patient variation. Data analysis was performed using one-way ANOVA with post-hoc Bonferroni test on the software Prism (Version 6.0, GraphPad Software, Inc). A p-value < 0.05 was considered statistically significant.

3. Results

3.1. hMSC Characterisation

First, morphologic characterization of isolated hMSCs in tissue culture flasts was performed. The first adherent cells were present by day 6 (**Figure 1**Ai), at which point non-adherent cells were removed (Figure 1Aii) and cells expanded until $\approx$90% confluence
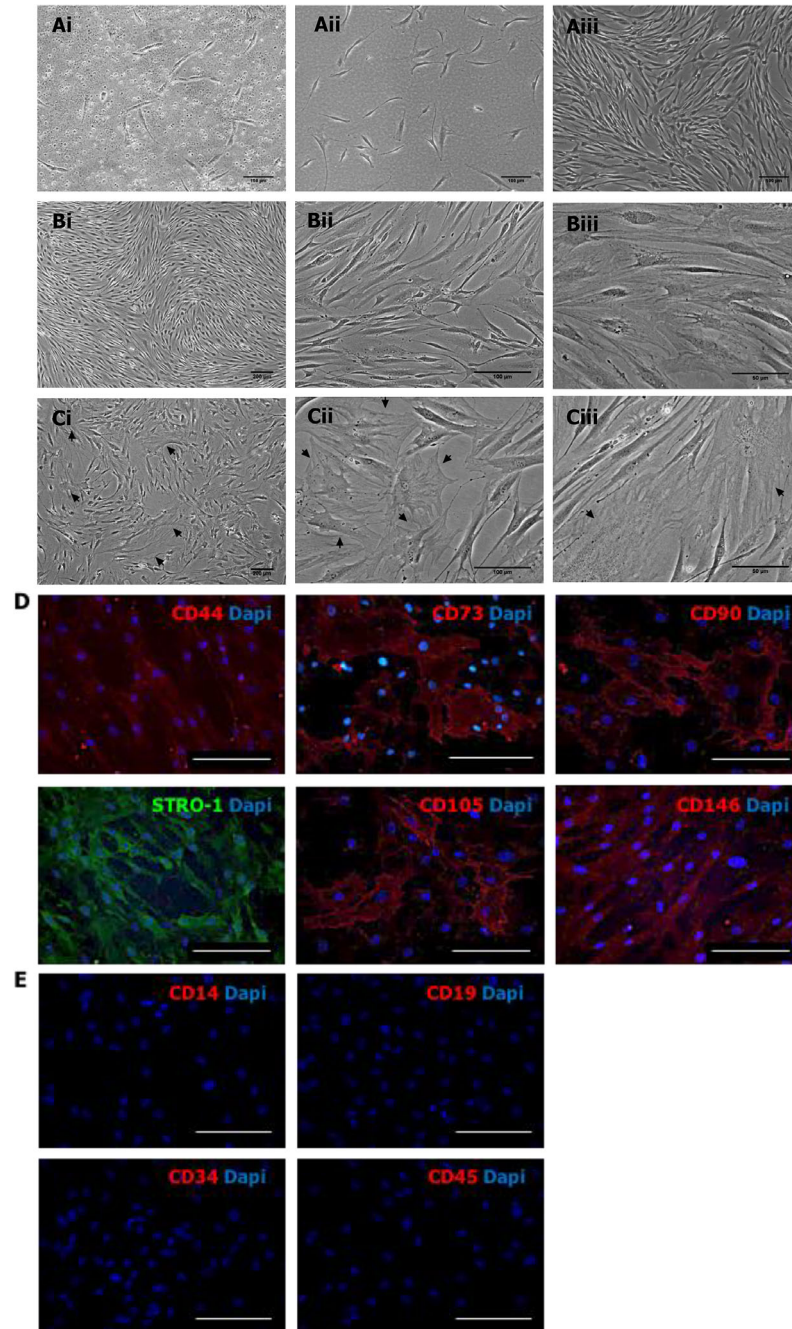
Figure 1. hMSC characterization. Morphology of thawed hMSCs at day 6 (Ai), in a mixture with hematopoietic non-adherent mononuclear cells. The latter were removed during medium exchange at day 6 (Aii). The hMSC monolayer became confluent after 21 days of culture (Aiii). At p2 (B) hMSCs exhibited the characteristic spindle-like, tapered shape. At p4 (C) hMSCs acquired an enlarged aspect and disorganized distribution in the flask. Black arrows indicate cells with enlarged morphology visible at p4. Immunphenotyping was performed to evaluate the expression of positive (D) and negative (E) hMSC cell surface markers on cells isolated from bone marrow aspirates. Flow cytometry was performed to validate the hMSC phenotype (F). Data are presented as the percentage of positive cells. The area shaded in lighter gray indicates the profile of the isotype controls. Histograms shown are representative of GX08 and GX09 batches. hMSCs multi-lineage differentiation ability was assessed for adipogenesis (Gi), chondrogenesis (Gii) and osteogenesis (Giii). Scale bars = 100 µm (Ai-iii, Bii, Cii, D, E), 200 µm (Bi, Ci), 50 µm (Biii, Ciii, Gi+iii), 2 mm (Gii).

**ADVANCED
SCIENCE NEWS**
www.advancedsciencenews.com

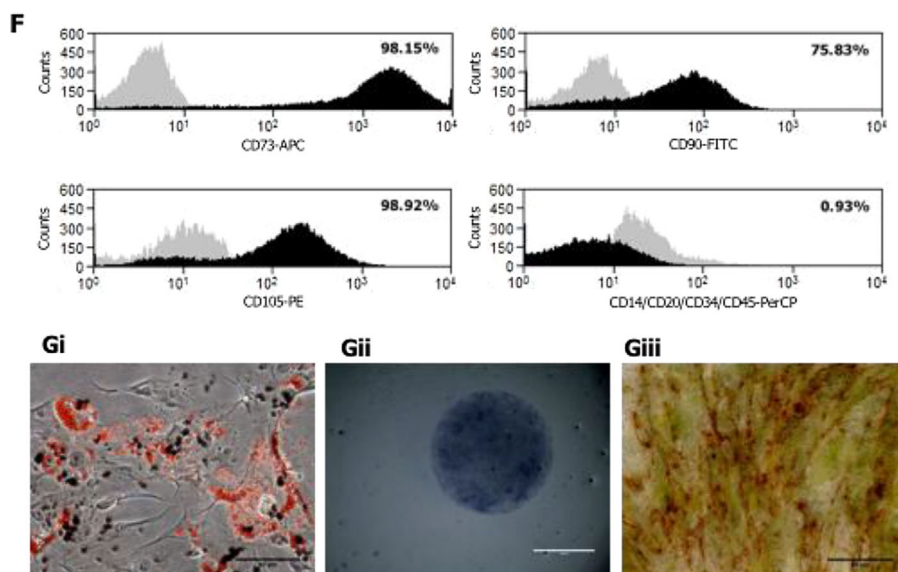**Biotechnology
Journal**
www.biotechnology-journal.com

Figure 1. Continued.

(Figure 1Aiii). Up to p3, all batches exhibited hMSC characteristic spindle-shaped morphology, with monolayers composed of tightly aligned cells (Figure 1Bi-iii). p4 cell morphology coincided with an increasing proportion of polygonal cells, exhibiting high cytoplasm-to-nucleus ratio and cytoplasmic filaments evidence. p4 cells also showed a disorganized spatial orientation (Figure 1Ci-iii).

Next, hMSC surface marker characterization was confirmed via immunofluorescence labeling using antibodies directed against CD44, CD73, CD90, CD 105, CD146, and STRO-1 antigen (positive markers, Figure 1D) and against CD14, CD19, CD34, CD45 (negative markers, Figure 1E). Flow cytometry was used to quantify expression using a reduced hMSC surface marker panel (Figure 1F), indicating that the cell population expressed markers associated to hMSCs (CD73: $98.15 \pm 2.25\%$; CD90: $75.83 \pm 9.12\%$; and CD105: $98.92 \pm 0.51\%$) and lacked markers associated with the bone marrow hematopoietic fraction (CD14, CD20, CD34, and CD45: $0.93 \pm 0.02\%$ combined expression).

Finally, in vitro multipotency ability of the batches was confirmed on p2 hMSCs, cultured under lineage-specific induction medium. Lipid vesicles became evident as early as day 9 in hMSCs grown in adipogenic medium. On day 14, Oil Red O staining revealed presence of numerous lipid compartments within the hMSC cytoplasm (Figure 1Gi). Chondrogenic differentiation was instead performed by culturing hMSC as micro-aggregates at a starting concentration of 1×10^7 cells/mL in chondrogenic medium. After 21 days, Alcian Blue staining determined positive proteoglycans synthesis by the micro-aggregates (Figure 1Gii). Finally, hMSCs under osteogenic culture conditions deposited calcified matrix as confirmed via positive Alizarin S staining (Figure 1Giii).

3.2. hMSCs Yield Per Passage

hMSC batches isolated from different donors were arbitrarily named GX01, GX02, GX03, GX04, GX05, GX06, GX07, GX08, X27, and X35. Monolayer cultures were serially passaged using a 1:3 splitting ratio. Growth kinetics was determined for each batch across five passages (p0–p4). **Figure 2** shows input and output averages of hMSC counts in T75 culture flasks. Inoculated cell amounts averaged $4.79 \times 10^5 \pm 3.97 \times 10^4$ total cells put into p1, $4.03 \times 10^5 \pm 5.34 \times 10^4$ into p2, $3.57 \times 10^5 \pm 6.22 \times 10^4$ into p3 and $3.26 \times 10^5 \pm 5.69 \times 10^4$ into p4, showing a decrease likely related to the non-fixed seeding density. However, the average hMSC number obtained from confluent monolayers decreased more significantly over passages: from $1.45 \times 10^6 \pm 1.25 \times 10^5$ at p0, to $1.22 \times 10^6 \pm 1.70 \times 10^5$ at p1, $1.04 \times 10^6 \pm 1.71 \times 10^5$ at p2, $9.33 \times 10^5 \pm 1.59 \times 10^5$ at p3, $7.47 \times 10^5 \pm 2.72 \times 10^4$ at p4, indicating an overall 48.5% average hMSC decrease from p0 to p4 expansion. Significant differences were observed between
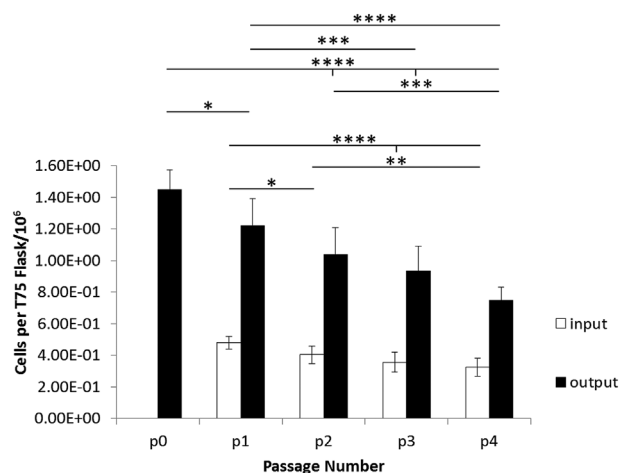

Figure 2. hMSCs were expanded according to a 1:3 splitting ratio. hMSCs yields of confluent monolayers (black bars) were calculated through Trypan Blue exclusion method before hMSCs suspensions were split and re-inoculated in the subsequent culture passage (white bars). $^*p = 0.0149$; $^{**}p = 0.0015$; $^{***}p < 0.001$; $^{****}\ p < 0.0001$.

**ADVANCED
SCIENCE NEWS**

www.advancedsciencenews.com

**Biotechnology
Journal**

www.biotechnology-journal.com

several groups but not between input hMSCs for p2 versus p3 and p3 versus p4, nor between output hMSCs for p1 versus p2 and p2 versus p3.

3.3. Achievable hMSC Density

To better evaluate hMSC expansion, cell density was documented for each batch once hMSCs reached confluency (**Figure** 3A and B). All hMSC batches showed a decrease in cell density, directly correlated to passage number increase. Average cell density was $1.93 \times 10^4 \pm 1.67 \times 10^3$ cells/cm^2 at p0, $1.63 \times 10^4 \pm 2.26 \times 10^3$ cells/cm^2 at p1, $1.38 \times 10^4 \pm 2.28 \times 10^3$ cells/cm^2 at p2, $1.24 \times 10^4 \pm 2.12 \times 10^3$ cells/cm^2 at p3, whereas the average yield was $9.96 \times 10^3 \pm 1.15 \times 10^3$ cells/cm^2 at p4.

This suggests a highly significant decrease between confluent hMSC cultures at passage 0 and at later culture passages (p0 vs. p1, p2, p3, and p4) as well as between p1 versus p3 and p4 and p2 versus p4. Figure 3C shows individual isolation data relative to the latter two passages, where modest inter-isolation variability is present, but again cell density differences between p2 and p3 from a same donor are negligible.

3.4. hMSC Proliferation and Expansion Potential

As directly correlated to cell proliferation, T_d was employed to elucidate hMSC growth rates. On average, the mean T_d for all batches equaled 94.36 ± 37.62 h to reach p1, 72.75 ± 31.55 h for p2, 60.55 ± 11.44 h for p3, and 77.39 ± 24.76 h for p4. The wide
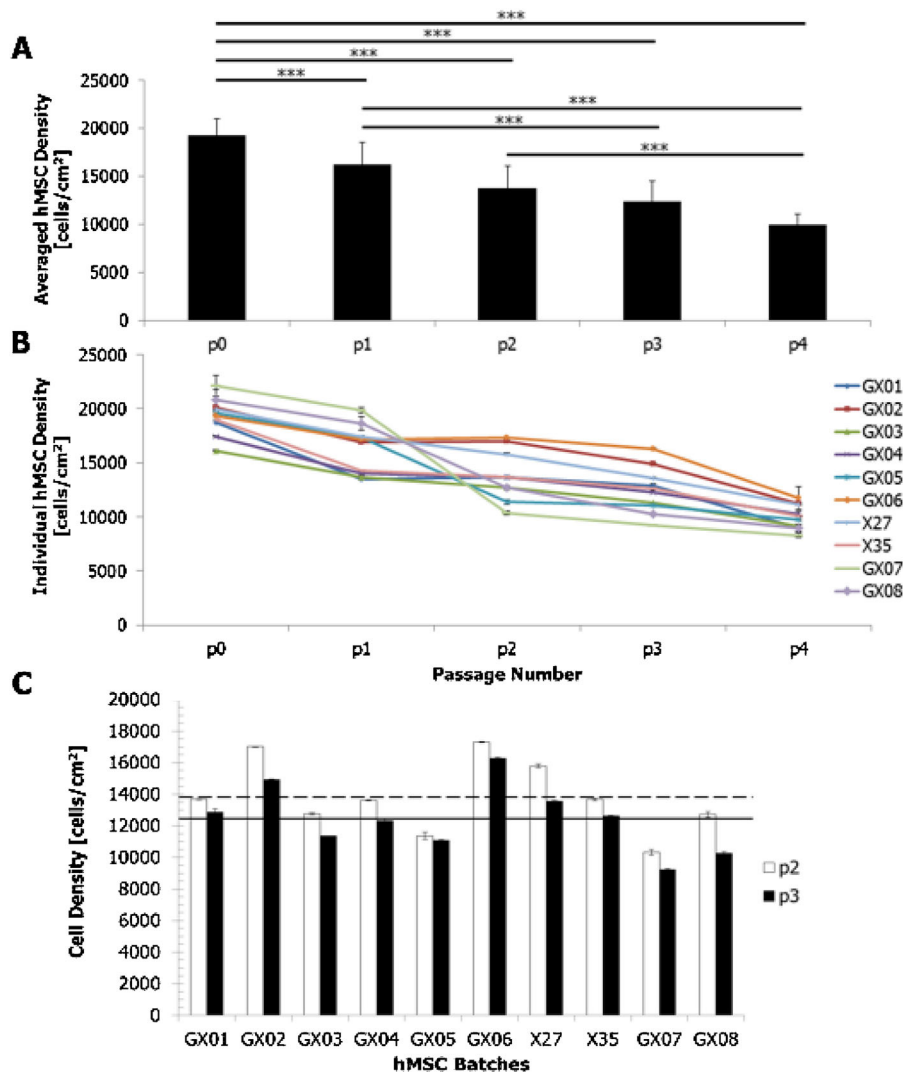

Figure 3. hMSC density over time in culture. Mean cell density significantly decreased with culturing time (indicated as passage number) in all cases except between p2 and p3 (A). Mean values were calculated from the cell density of each hMSC batch across five passages (B). When comparing densities at p2 and p3, hMSC cultures exhibited higher density at p2 than at p3 (C). This was observed in all isolations expanded, but no significant difference was present between p2 and p3 hMSCs from a same donor. Mean p2 value $= 1.38 \times 10^4$ hMSCs/cm^2 (dashed line); mean p3 value $= 1.24 \times 10^4$ hMSCs/cm^2 (bold line). *** $p < 0.001$.

**ADVANCED
SCIENCE NEWS**
www.advancedsciencenews.com

**Biotechnology
Journal**
www.biotechnology-journal.com

variation observed across batches resulted in no statistically significant differences across mean T_d values for each passage. The highest T_d to reach p2 was exhibited by GX06, GX07, GX05, and GX08: this reflects a slower growth rate at p2 for these batches, although their T_d fell closer to the rest of the batches at p3 (**Figure 4**A).

To further analyze hMSC growth rates, additionally to "passage" analysis, hMSC counts were used to determine the population doubling level (PDL) for all batches. PDL curves (Figure 4B) better represent the cell growth rate and the in vitro age than passage number, and its steady increase through expansion indicated that hMSCs proliferated sustainably across all passages considered, with all batches reaching an average PDL$\approx$12 at p4. Although PDL values were comparable at each passage for each batch, the time required varied. The slowest growth rate in terms of PDL over culturing time was in GX01, GX07, and GX08.

Serial passage (**Figure 5**A) and population fold increase in cell number (Figure 5B) across the five passages was calculated for all hMSC batches. Seven batches displayed the highest serial passage fold increase at p2, followed by p3, but we observed three out of ten outliers (GX05, GX07, and GX08) for which this was not true. Nevertheless, the overall trend across adjacent passages for hMSC isolated from individual donors was consistent with the observation of overall population fold increase in cell number, where the same outliers were identified. Of note, no statistically significant differences were detected in overall fold increase in cell number between donors.

Predicted hMSC expansion potential was measured as a relationship of the total achievable yield after each passage over time in culture. Individual expansion values are expressed in Figure 5C. Total yields were deduced from the hMSC density previously calculated, accounting for the 1:3

passage ratio which would be used for hMSC re-seeding at each passage. Figure 5D presents the average expansion yields for all batches, with p0 yielding on average $\approx$2.82 $\times 10^6 \pm 2.03 \times 10^5$ hMSCs, p1$\approx$6.23 $\times 10^6 \pm 1.75 \times 10^6$, p2$\approx$17.29 $\times 10^6 \pm 5.19 \times 10^6$, p3$\approx$50.40 $\times 10^6 \pm 8.59 \times 10^6$, and p4$\approx$121.01 $\times 10^6 \pm 13.9 \times 10^6$. These data, together with the previous on actual growth kinetics, allowed us to conclude that a positive proliferation and expansion potential intrinsically characterized all ten hMSC batches at least until the completion of passage 4, but also that cell size and morphology vary substantially with cell expansion.

4. Discussion

This study describes the expansion and achievable hMSC yields from a pool of 10 different bone marrow young male donors aged 16–18 years old. The goal was to characterize growth kinetics of healthy baseline "reference" hMSCs using typical manual processing. The actual patient populations requiring hMSC therapies will likely be of wide age range and suffer from illness, so inter-patient variability in quality of cell material will result from age and disease status. Other sources of variability in hMSC quality arise from variability in isolation and processing protocols.[15] Therefore, the rationale underlying our work was to address observe process variability independent of donor age and gender.

Although some hMSC culture strategies can employ fixed low seeding density to limit senescence onset,[16,17] here we used a fixed splitting ratio (1:3) typically used for primary somatic cell cultures. hMSCs from all batches displayed morphology typical of early progenitors[18] when maintained in culture until the end of p3. Notably, although no significant differences were detected, the lowest T_d was observed for p3 cultures (PDL$\approx$8–10), suggesting that, overall, at this stage hMSCs had the fastest growth rate.

When hMSCs are expanded in vitro, they are affected by processing variables, including cell seeding density and oxygen tension,[19] and also encounter replicative senescence[20] due to loss of the physiologic niche where they resided quiescent. In vitro culture conditions (e.g., plastic adhesion, exposure shear forces during pipetting, media reagents, detaching enzymes, etc.) can accelerate aging and loss of function.[21,22] Strategies to limit senescence and loss of functionality include processing under reduced oxygen tension[23] or in presence of growth factors such as FGF-2,[24,25] as was performed in this study.

Even when employing a fixed seeding density for primary cells at p0, we measured a substantial amount of variability in the time taken to initiate cell doublings, likely reflecting variability in hMSC viability at seeding. This may be further affected if the cells are cryopreserved, as was the case in this study . Critically, cell identity markers need to be at a consistently acceptable level. The ten batches processed displayed hMSC markers, although CD90 showed some variability relative to the other markers, suggesting that it may be a critical marker of product quality. Indeed, CD90 expression was demonstrated to regulate hMSC differentiation ability.[26] However, this did not appear to impact on any of the donor hMSC's ability to undergo tri-lineage differentiation.
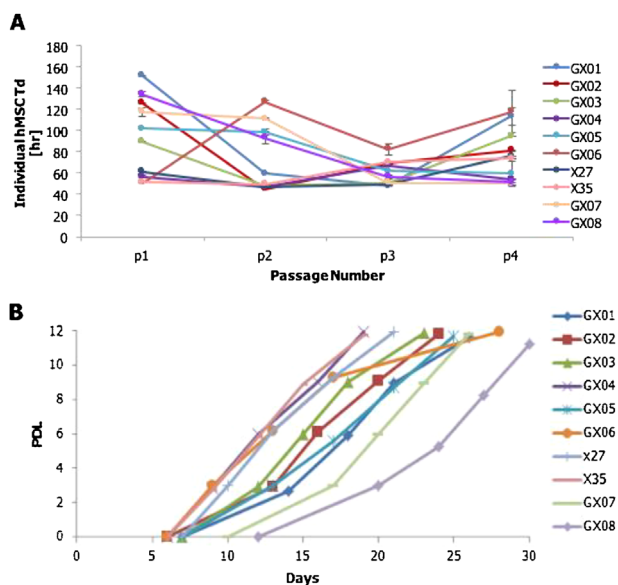

Figure 4. hMSC doubling time population doublings achieved across serial passages. Td curves between passages were calculated for each hMSC batch across the four passages (A) and cumulative population doubling level (PDL) was assessed for each donor over time up to passage 4 and was based on initial cell input and total cell output (B).
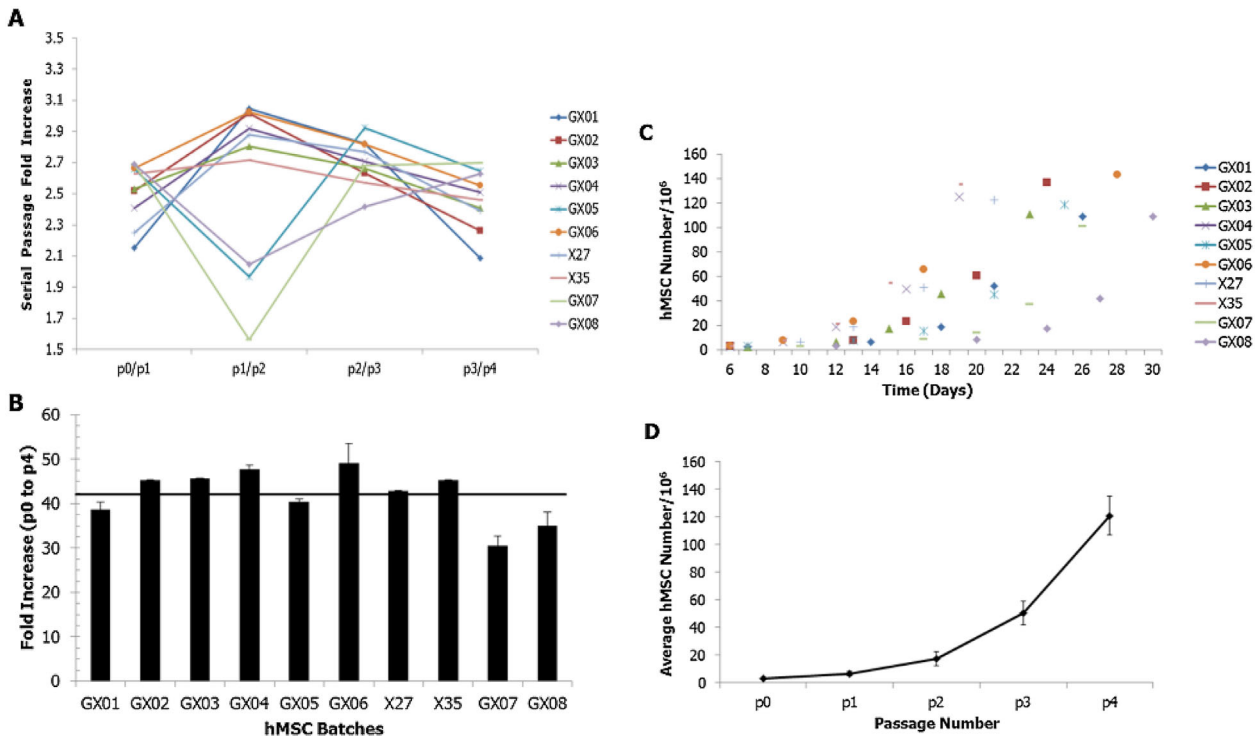
**ADVANCED
SCIENCE NEWS**
www.advancedsciencenews.com

**Biotechnology
Journal**
www.biotechnology-journal.com

Figure 5. Fold increase in cell number and expansion potential of start population. Fold increase in cell number between serial passages was consistent for all the hMSC batches isolated except for GX05, GX07, and GX08 (A). Overall fold increase across five passages, from p0 and p4, is shown for all hMSC batches (B), where the mean across donors was 42.06 (bold line). No statistical differences were detected between hMSC batches. Expansion potential across five passages was calculated for each individual donor (C) and averaged across donors (D).

The decrease in cell density at harvest correlated with morphological observation of cell enlargement at p4 (PDL > 10, $T_d \approx 77.3$ h) for all batches, likely due to in vitro cell aging. This corroborates a recent report by Whitfield et al.,[27] who reported hMSC size increase over time due to exit from the cell cycle. Statistically significant differences in cell density ($p < 0.001$) were observed between p4 versus p0 and p1 (PDL ≈ 2.9, $T_d \approx 94$ h), confirming that cells slow and become senescent over time and that the number of rapidly dividing progenitors was dramatically reduced by p4 compared with previous passages. However, PDL measurements indicate that hMSCs expansion was faster between p1 and p3 (PDL ≈ 8.8, $T_d \approx 60$ h), so the decreasing output cell yields recorded are presumably also partly a function of increased passage frequency. hMSCs from three donors (GX05, GX07, and GX08) exhibited a more pronounced drop in cell density between p1 and p2, possibly because of earlier onset of senescence in these batches because of more rapid maturation in culture. In fact, it was between p1 and p2 (PDL ≈ 5.8, $T_d \approx 72$ h) that the most heterogeneous fold increase in cell number was noted across batches and hence where process monitoring and control is most likely needed to identify potential failures earlier in the process. This could be achieved by implementing in-process monitoring that could include real-time morphology assessment, time-lapse documentation of population dynamics and off-line monitoring of metabolites.

Nevertheless, in this study PDL and fold increase in cell numbers from p0 to p4 indicated constant growth of hMSCs from all donors. Interestingly, two of the three outliers (GX07

and GX08) for cell density between p1 and p2 had the slowest growth rates as measured via PDL, and consequently the estimated proliferation potential of the population might be substantially impaired compared to the other batches. This observation also correlated with a longer doubling time required for the two outliers to reach p3.

Donor age and gender may both impact on hMSC proliferation ability. It has been recently reported that bone marrow-derived hMSCs originating from young (<45 years old) female donors have a slight but significantly reduced T_d compared to young male donors.[28] Using hMSCs isolated from relatively young male donors, we measured cell proliferation ability via PDL, representing the number of total population doublings since their initiation in vitro. It is clear that assessing either PDL or T_d in hMSCs isolated from young donors will provide a real measure of which cultures possess higher expansion potential in vitro.[13,20,28–30] Based on the cell density, PDL and fold increase data, at p2 and p3 young male donor hMSCs share similar growth kinetics profiles. Finally, expansion potential was calculated for the different hMSC isolations up to p4 to determine theoretical yield of cells that could be achieved. The highest yield measured among all ten batches at p2 and p3 was almost twice (GX06, p2 $\approx 2.33 \times 10^7$ cells/cm^2 and p3 $\approx 6.59 \times 10^7$ cells/cm^2) the lowest yield obtained (GX07, p2 $\approx 1.39 \times 10^7$ cells/cm^2 and p3 $\approx 3.74 \times 10^7$ cells/cm^2), indicating the variability range of hMSC yields that might be expected for the generation of autologous cell therapy products.

**ADVANCED
SCIENCE NEWS**

www.advancedsciencenews.com

**Biotechnology
Journal**

www.biotechnology-journal.com

All ten independent donor hMSCs characterized for growth potential in this paper displayed similar growth kinetics profiles in terms of declining achievable density at harvest. This suggests that defining a process operating window based on a representative range of healthy donor samples should be feasible to enable expansion of autologous cells for therapy using manual processing. If manufacturing predictions on the range of achievable hMSC yields can be made early in the expansion phase, that is, in a p1–p3 operating window (PDL < 10), then overall resource requirements and process risks can be reduced for both industry and patient benefit. The degree of heterogeneity between batches from p1 to p2 observed in this study indicates that it may be feasible to predict success or failure earlier on in the process. However, the current data, at $n = 10$, represents a relatively small sample size and therefore greater numbers of primary hMSC batches would need to be tested to validate these observations.

hMSC expansion potential is critical for achieving clinical scale. In this context, the real challenge is achieving clinically relevant cell numbers before hMSC progenitor phenotype is lost beyond passage 4. Our data show that by expanding hMSCs with standard protocols outlined in this study, p2 and p3 cells could give rise to early-progenitor hMSCs populations that could be expanded for clinical applications. However, development of functional tests to define mode of action, for example, paracrine signaling, vascular support, is required to confirm cell product quality.

Nevertheless, as the process is brought toward product development, the expansion requirements can dramatically increase to reach adequate clinical levels. By taking cardiovascular diseases as an exemplar due to their incidence and lethality worldwide, there is a small body of literature on early-phase clinical studies assessing autologous hMSCs for therapeutic potency in MI patients.[31–35] Although these studies are different in a variety of parameters, such as patient inclusion criteria, cell delivery method as well as outcome measurements, the total cell number infused per dose was never lower than 5×10^6. Where cells in the order of 10^6–10^7 are required, the processing strategies reported here, that can yield on average 17×10^6 cells at p2 and 50×10^6 at p3, would appear to be an attractive route forward. However, in the POSEIDON trial[35] the greatest therapeutic benefit was seen with multiple administrations of 20×10^6 hMSCs per dose and this suggests, along with other estimates[36] that up to 10^8 cells per patient will be required.

It can be assumed that with a single 4-layer cell factory ($2528\,cm^2$ cell expansion surface) a 33-fold increase in hMSC yield (compared to a T75 flask) can be achieved. Also, multilayer flasks reduce manual processing needs. However, moving toward 10^8 cells per dose, it is not clear whether cell quality would be maintained and so robust identity and functional hMSC characterization tools, that to date are still lacking, will be essential to better understand potency of the cells and differences in potency between individual patients.

Abbreviations

DAPI, 4′,6-diamidino-2-phenylindole; EDTA, thylenediaminetetraacetic acid; hMSC, human mesenchymal stromal cell; PBS, phosphate buffer saline; PDL, population doubling level; PFA, paraformaldehyde; T_{d}, doubling time.

Conflict of interest

The authors declare no financial or commercial conflict of interest.

[1] A. I. Caplan, S. P. Bruder, *Trends Mol. Med.* **2001**, *7*, 259.

[2] A. I. Caplan, *J. Cell Physiol.* **2007**, *213*, 341.

[3] M. F. Pittenger, *Science* **1999**, *284*, 143.

[4] K. Mareschi, D. Rustichelli, R. Calabrese, M. Gunetti, F. Sanavio, S. Castiglia, A. Risso, I. Ferrero, C. Tarella, F. Fagioli, *Stem Cells Int.* **2012**, *2012*, 1.

[5] P. J. Psaltis, S. Paton, F. See, A. Arthur, S. Martin, S. Itescu, S. G. Worthley, S. Gronthos, A. C. W. Zannettino, *J. Cell. Physiol.* **2010**, *223*, 530.

[6] P. Bianco, X. Cao, P. S. Frenette, J. J. Mao, P. G. Robey, P. J. Simmons, C.-Y. Wang, *Nat. Med.* **2013**, *19*, 35.

[7] M. Dominici, K. Le Blanc, I. Mueller, I. Slaper-Cortenbach, F. Marini, D. Krause, R. Deans, A. Keating, D. Prockop, E. Horwitz, *Cytotherapy* **2006**, *8*, 315.

[8] R. Zohar, J. Sodek, C. A. McCulloch, *Blood* **1997**, *90*, 3471.

[9] P. J. Simmons, B. Torok-Storb, *Blood* **1991**, *78*, 55.

[10] D. T. Covas, R. A. Panepucci, A. M. Fontes, W. A. Silva, M. D. Orellana, M. C. C. Freitas, L. Neder, A. R. D. Santos, L. C. Peres, M. C. Jamur, M. A. Zago, *Exp. Hematol.* **2008**, *36*, 642.

[11] A. Tormin, O. Li, J. C. Brune, S. Walsh, B. Schütz, M. Ehinger, N. Ditzel, M. Kassem, S. Scheding, *Blood* **2011**, *117*, 5067.

[12] J. Kim, J. W. Kang, J. H. Park, Y. Choi, K. S. Choi, K. D. Park, D. H. Baek, S. K. Seong, H.-K. Min, H. S. Kim, *Arch. Pharm. Res.* **2009**, *32*, 117.

[13] M. M. Bonab, K. Alimoghaddam, F. Talebian, S. H. Ghaffari, A. Ghavamzadeh, B. Nikbin, *BMC Cell Biol.* **2006**, *7*, 14.

[14] L. Sensebé, P. Bourin, K. Tarte, *Hum. Gene Ther.* **2011**, *22*, 19.

[15] V. Tanavde, C. Vaz, M. S. Rao, M. C. Vemuri, R. R. Pochampally, *Cytotherapy* **2017**, *17*, 1169.

[16] B. Neuhuber, S. A. Swanger, L. Howard, A. Mackay, I. Fischer, *Exp. Hematol.* **2009**, *36*, 1176.

[17] E. Fossett, W. S. Khan, *Stem Cells Int.* **2012**, *2012*, 1.

[18] I. Sekiya, B. Larson, J. Smith, R. Pochampally, J. Cui, D. Prockop, *Stem Cells* **2002**, *20*, 530.

[19] F. DosSantos, P. Z. Andrade, J. S. Boura, M. M. Abecasis, C. L. da Silva, J. M. S. Cabral, *J. Cell. Physiol.* **2010**, *223*, 27.

[20] A. Banfi, G. Bianchi, R. Notaro, L. Luzzatto, R. Cancedda, *Tissue Eng.* **2002**, *8*, 901.

[21] M. Pevsner-Fischer, S. Levin, D. Zipori, *Stem Cell Rev.* **2011**, *7*, 560.

[22] M. E. Bernardo, N. Zaffaroni, F. Novara, A. M. Cometa, M. A. Avanzini, A. Moretta, D. Montagna, R. Maccario, R. Villa, M. G. Daidone, O. Zuffardi, F. Locatelli, *Cancer Res.* **2007**, *67*, 9142.

[23] L. Basciano, C. Nemos, B. Foliguet, N. de Isla, M. de Carvalho, N. Tran, A. Dalloul, *BMC Cell Biol.* **2011**, *12*, 12.

[24] Y. W. Eom, J.-E. Oh, J. I. Lee, S. K. Baik, K.-J. Rhee, H. C. Shin, Y. M. Kim, C. M. Ahn, J. H. Kong, H. S. Kim, K. Y. Shim, *Biochem. Biophys. Res. Commun.* **2014**, *445*, 16.

[25] G. Bianchi, A. Banfi, M. Mastrogiacomo, R. Notaro, L. Luzzatto, R. Cancedda, R. Quarto, *Exp. Cell Res.* **2003**, *287*, 98.

[26] D. A. Moraes, T. T. Sibov, L. F. Pavon, P. Q. Alvim, R. S. Bonadio, J. R. Da Silva, A. Pic-taylor, O. A. Toledo, L. C. Marti, R. B. Azevedo, D. M. Oliveira, *Stem Cell Res. Ther.* **2016**, *90*, 1.

[27] M. J. Whitfield, W. C. J. Lee, K. J. Van Vliet, *Stem Cell Res.* **2013**, *11*, 1365.

[28] G. Siegel, T. Kluba, U. Hermanutz-Klein, K. Bieback, H. Northoff, R. Schäfer, *BMC Med.* **2013**, *11*, 146.

[29] K. Stenderup, *Bone* **2003**, *33*, 919.

[30] A. Madeira, C. L. da Silva, F. dos Santos, E. Camafeita, J. M. S. Cabral, I. Sá-Correia, *PLoS ONE* **2012**, *7*, 43523.

[31] S. Chen, W. Fang, F. Ye, Y.-H. Liu, J. Qian, S. Shan, J. Zhang, R. Z. Chunhua, L. Liao, S. Lin, J. Sun, *Am. J. Cardiol.* **2015**, *94*, 92.

[32] S. F. Rodrigo, J. van Ramshorst, G. E. Hoogslag, H. Boden, M. A. Velders, S. C. Cannegieter, H. Roelofs, I. Al Younis, P. Dibbets-Schneider, W. E. Fibbe, J. J. Zwaginga, J. J. Bax, M. J. Schalij, S. L. Beeres, D. E. Atsma, *J. Cardiovasc. Transl. Res.* **2013**, *6*, 816.

[33] S. Chen, Z. Liu, N. Tian, J. Zhang, F. Yei, B. Duan, Z. Zhu, S. Lin, T. W. Kwan, *J. Invasive Cardiol.* **2006**, *18*, 552.

[34] M. Mohyeddin-Bonab, M. R. Mohamad-Hassani, K. Alimoghaddam, M. Sanatkar, M. Gasemi, H. Mirkhani, H. Radmehr, M. Salehi, M. Eslami, A. Farhig-Parsa, H. Emami-Razavi, M. Ghasemi al-Mohamad, A. A. Solimani, A. Ghavamzadeh, B. Nikbin, *Arch. Iran. Med.* **2007**, *10*, 467.

[35] V. Y. Suncion, E. Ghersin, J. E. Fishman, J. P. Zambrano, N. Mandel, K. H. Nelson, G. Gerstenblith, D. L. Difede, E. Breton, K. Sitammagari, I. H. Schulman, N. Taldone, A. R. Williams, C. Sanina, P. V. Johnston, J. Brinker, P. Altman, M. Mushtaq, B. Trachtenberg, A. M. Mendizabal, J. Da Silva, I. K. Mcniece, A. C. Lardo, R. T. George, M. Hare, A. W. Heldman, *Circ. Res.* **2014**, *114*, 1292.

[36] A. S. Simaria, S. Hassan, H. Varadaraju, J. Rowley, K. Warren, P. Vanek, S. S. Farid, *Biotechnol. Bioeng.* **2014**, *111*, 69.